

CHEMICAL REACTIONS AND LASERS: ELEMENTARY STEPS AND COMPLEX SYSTEMS

J. Wolfrum

Physikalisch-Chemisches Institut der Universität, Im Neuenheimer Feld 253, 6900 Heidelberg, FRG

Abstract

In recent years, various methods have been developed to observe and to influence the course of chemical reactions using laser radiation. By selectively increasing the translational, rotational, and vibrational energies of the reaction partners with high intensity visible and UV lasers, direct insight can be gained into the molecular course of the breaking and re-forming of chemical bonds.

The production of free radicals by laser radiation can be used in chemical synthesis for the production of monomers. As example the kinetics of the UV-laser induced dehydrochlorination of CH_2CClF_2 is described.

The application of linear and non-linear laser spectroscopic methods allows a non-intrusive observation of the interaction of transport processes with chemical reactions used with high temporal, spectral and spatial resolution. As a simple test system the ignition of O_2 - O_3 mixtures by irradiation with a CO_2 laser along the axis of a cylindrical vessel is considered. Mathematical simulation of the ignition process is simulated mathematically by solving the corresponding system of conservation equations. Experimental data are presented for velocity components of the flame front from IR-UV double resonance experiments and for the temperature history from infrared absorption measurements using tunable diode lasers.

1. INTRODUCTION

The strong dependence of the rate of chemical reactions on the energy supplied is one of the most important observations for the chemist. Often, the energy of the reaction partners can be represented by one temperature. The dependence of the reaction rate on temperature is described by the now exactly hundred years old Arrhenius equation /1/. The Arrhenius parameters obtained in this way do not, however, provide any information on the respective contribution of the degree of freedom of the participating reaction partners in overcoming the energy barrier of the reaction. In the following examples, reactions in the gas phase are used to show how information on microscopic details of breaking and re-forming of bonds in chemical reactions can be obtained in experiments with lasers.

Mostly Hg- or Xe-lamps are used as light sources for industrial photochemistry. Laser photons have to compete both in investment and operational cost as well as in maintenance expenditure, long term power, and lifetime. For economic application of lasers in this area, the effective cost of the photons produced must lie considerably below that for the desired product. One should remember that generally, the product price is determined only to a small extent by the photochemical step involved in the production and that techniques employing lasers have to compete not only with a conventional photochemical processes, but also with other routes of synthesis. Optimally, the use of lasers should result in several improvements simultaneously, such as cheaper starting materials, fewer or more valuable side products, and fewer or cheaper process steps. In particular, the production of cheap mass-produced chemicals by the use of lasers is only worthwhile if very high quantum yields (number of product molecules produced per photon generated) can be achieved in radical chain reactions. As an example, experiments on the kinetics of the UV-laser induced dehydrochlorination of 1-chloro-1,1-difluoroethane will be discussed.

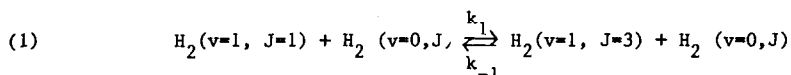
Laser spectroscopy can provide non-intrusive observation of rapidly changing chemical reactions, such as combustion processes, with high temporal, spectral, and spatial resolution. In the last part of this contribution the application of laser techniques to observe and to stimulate ignition processes is described.

2. MICROSCOPIC DYNAMICS OF ELEMENTARY CHEMICAL REACTIONS

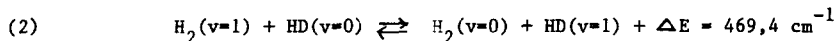
2.1 Laser Rotational and Vibrational Excitation

The reaction of hydrogen molecules with hydrogen atoms or their isotopes, as the simplest example of a bimolecular reaction of neutral particles, is particularly suitable for a theoretical investigation of the influence of selective excitation of reacting species. The energy of one vibrational quantum of the hydrogen molecule considerably exceeds the Arrhenius activation energy (E_a), the threshold energy (E_0) as well as the height of the potential energy barrier (E_c) of the reaction in the vibrational ground state. E_c was first calculated quantum mechan-

cally by London /2/ more than half a century ago. Classical methods for the study of reaction kinetics are difficult to apply to this reaction, because known concentrations of vibrationally excited hydrogen molecules have to be produced and detected. Due to the lack of a dipole moment and an electronic absorption spectrum in the vacuum ultraviolet, state-selective studies using spectroscopic methods were difficult to perform for a long time, before laser methods became available. Fig. 1 shows the excitation and detection scheme of a laser experiment for energy transfer and state selective reaction studies of hydrogen molecules. Stimulated Raman pumping is employed to populate $H_2(v'' = 1, J'' = 1)$ selectively in the electronic ground state of hydrogen within a 10ns laser pulse. The time-dependent populations in rotational and vibrational levels in hydrogen and isotopic modifications can be probed by coherent anti-Stokes Raman spectroscopy (CARS). In the experimental arrangement /3/ 50% of the energy output of a linearly polarized frequency-doubled Nd:YAG laser (Quanta Ray DCR1A, at 532 nm) is focussed into a Raman cell containing a hydrogen-helium mixture with partial pressures of 20 bar and 10 bar respectively. The helium is used to reduce the pressure-dependent line shift of the Stokes line. Stimulated Stokes Raman radiation is generated in forward and backward directions. Due to the phase conjugation effect in stimulated Raman-scattering, the backward beam displayed a more homogeneous intensity distribution over the beam cross section and a smaller divergence than the forward scattered beam. Both beams are focussed into the centre of the reaction cell with a beam waist of about 200 μm diameter for both fundamental and Stokes beams. The rate constants obtained from this experiment for the relaxation processes

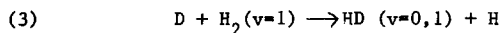


of $k_1 = 2,2 \times 10^{-12}$ (cm^3/s) and $k_{-1} = 1,4 \times 10^{-11}$ (cm^3/s) are in good agreement with measurements using LIF-Spectroscopy in the VUV spectral region for $H_2(v, J)$ detection /4/. In a similar way the vibrational energy transfer from $H_2(v=1)$ molecules can be studied. The diffusion of excited H_2 and HD out of the CARS beam strongly influences the time evolution of the CARS signal. To estimate the influence of diffusion, an analytical expression for the solution of the kinetic equations coupled with transport processes is required. From such modelling calculations the rate constants for the vibrational energy exchange processes



of $k_2 = 1,9 \times 10^{-13}$ (cm^3/s) in the exothermal and $k_{-2} = 1,4 \times 10^{-14}$ (cm^3/s) in the endothermal direction are obtained.

The CARS detection system provides an ideal method for monitoring directly reactants and products in different vibrational states /5/ in the reaction



The reaction is followed in a discharge flow system (3), where the atoms and $H_2(v=1)$ molecules were generated by microwave discharges (see Fig. 2). HD($v=1$) and HD($v=0$) molecules can be formed in adiabatic and non-adiabatic reaction pathways in this reaction. In the experiment the formation of HD($v=1$) as function of time (see Fig. 3) shows the competition of the production in the adiabatic channel of reaction (3) and the removal by vibrational energy transfer by step (-2). The experimental results obtained so far indicate a significant predominance of the adiabatic over the non-adiabatic reactive pathways (see Fig. 4). The experiments also show that when the H_2 molecule is excited to the first vibrational state, only about a third of the vibrational energy is used to overcome the potential energy barrier E . Thus, the reaction of vibrationally excited hydrogen molecules still shows an energy barrier, whose height can be predicted both from classical and from quantum mechanical calculations of the course of reaction on the "ab initio" potential surface. As shown in the Arrhenius diagram of Fig. 4 only at low temperatures significant differences between classical and quantum predictions of the reaction rate can be expected. Such experiments are underway at the moment in our laboratory.

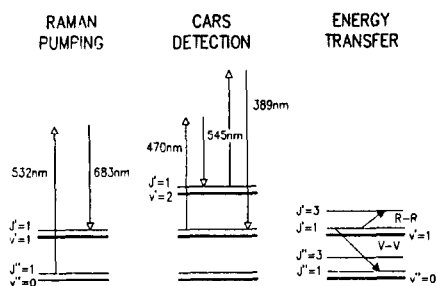


Fig. 1 Energy level diagram for the excitation and detection of state-selected hydrogen molecules by Raman and CARS spectroscopy

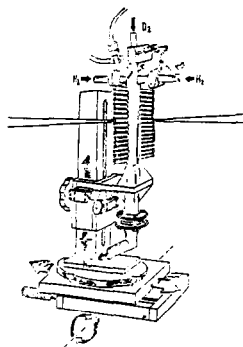


Fig. 2 Discharge flow system for investigation of the reaction $D + H_2(v=1) \rightarrow HD(v=1,0) + H$ by CARS spectroscopy

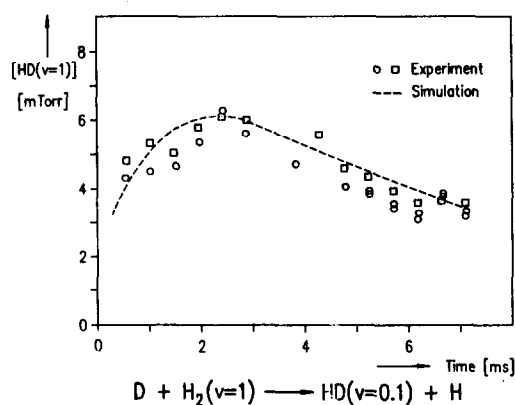
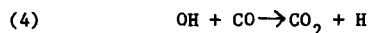


Fig. 3 CARS measurements of the HD ($v=1$) formed in the $D + H_2$ ($v=1$) reaction

2.2 Laser Translational Excitation

The reaction



is a dominant step for conversion of CO into CO_2 in combustion systems and in the chemistry of the upper atmosphere. Various measurements of the thermal rate constants over a wide temperature range ($200K < T < 2500K$) show an upward curvature of the Arrhenius plot. Transition-state theory explains the curvature in the $\ln k$, versus $1/T$ plot by using different activated complex configurations and barrier heights in the exit channel. Measurements with state selected reactants should give more microscopic details of the reaction for comparison with dynamic simulations. A rate enhancement of less than a factor 2 was measured after vibrational excitation of OH /6/, while vibrational excitation of CO even results in a decrease of the rate coefficient /7/. Early work on reaction (-4) with translationally excited reactants was performed with H atoms produced by flash-light photolysis of HI and detection of CO by gas chromatography /8,9/. Due to the poor time resolution and the broad H-atom velocity distribution in this experiment, only overall reaction probabilities could be given. Laser photolysis of H donors like hydrogen halogenides or H_2S yields well-defined translationally excited H atoms. The first laser-photolysis studies on H + CO_2 were not on reactive collisions but on collision-induced vibrational excitation of CO_2 /10,11/. Laser photolysis of HBr and laser-induced fluorescence (LIF) detection of OH produced by reaction (-4) was first reported by Quick and Tsee /12/, but pressure and delay time did not allow a measurement of the nascent OH population. Kleinermaans et al. /13,14/ determined rotational energy distribution at 1.9 and 2.6 eV collision energy and an absolute reactive cross sections for reaction (-4). In addition several papers were published on H + CO_2 experiments in molecular beams using van der Waals "precursor molecules" /15,16/, where time-resolved measurements on the pico- and femto-second scale were reported /17/. Although the results may look very similar in both types of experiment, comparison is difficult due to geometrical restriction of the collision in dissociating van der Waals complexes. A comprehensive paper on hot H-atom activities was published by Flynn and Weston /18/.

The dynamics of elementary reactions with a high energy barrier can be studied in microscopic detail by combining translationally hot atom formation from laser photolysis with time-state and orientation-resolved product detection by laser-induced fluorescence spectroscopy. The apparatus /19/ is depicted in Fig. 5. Two laser beams are directed perpendicularly through a flow reactor equipped with long side arms to reduce the scattered light from the dye laser analysis pulse. Fluorescence light is detected as a function of the dye laser wavelength through emission optics and a filter by a photomultiplier. Keeping the probe laser wavelength fixed on the centre of an OH transition, OH time profiles could be recorded by scanning the probe laser and boxcar gate synchronously against the fixed photolysis pulse. Additionally, keeping the photolysis and probe pulse fixed in time and scanning the delay between the probe laser and the narrow boxcar gate (5ns), the measured exponential decrease of the OH fluorescence was used to determine the fluorescence lifetime.

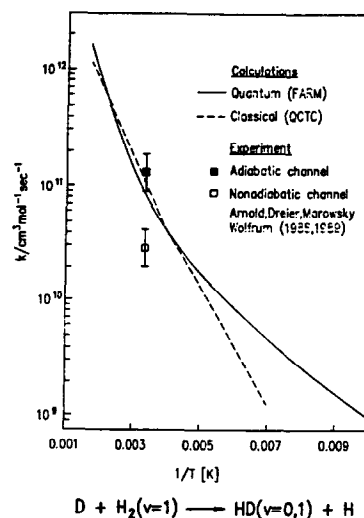


Fig. 4 Arrhenius diagram for the temperature dependence of the rate for the reaction $D + H_2$ ($v=1$) \rightarrow HD ($v=0,1$) + H

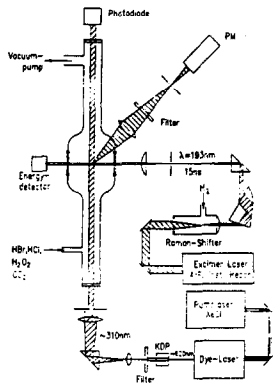


Fig. 5 Experimental arrangements for the study of the reactions with translationally hot atoms and radicals by combination of excimer laser photolysis and LIF product detection

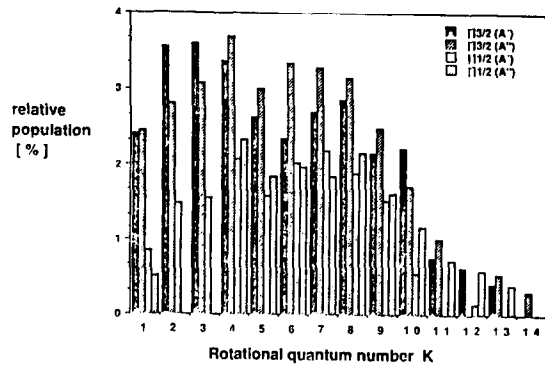


Fig. 6 OH ($v=0$) rotational population distribution for the reaction $H(1.86 \text{ eV}) + \text{CO}_2 \rightarrow \text{CO} + \text{OH}$

The rotational distribution found for all fine structure components of OH ($v=0$) is shown in Fig. 6. Levels up to $K = 14$ are populated with a maximum population at $K = 3-7$ and an average $K = 6$. The lower-energy spin-orbit component OH($^2\Pi_{3/2}$) is more populated than the higher-energy component OH($^2\Pi_{1/2}$). For both spin orbit components A' (unpaired electron orbital lobes in the plane of the molecular rotation) and A'' (unpaired electron orbital lobes perpendicular to the plane of rotation) /20/ are found to be equally populated. The lambda doublet ratio for OH ($v=0$) is constant at 0.98 ± 0.17 independent of N . The formerly published ratio of $A'/A'' = 3 + 1$ at 2.6 eV /14/ has recently been remeasured under unsaturated conditions and corrected to a statistical distribution /21/.

The initial rotational distribution for the first vibrationally excited state was also determined. The vibrational branching ratio for reaction of 1.86 eV H atoms with CO_2 is 0.06 ± 0.02 . Kleinermaas et al. /22/ introduced a method of determining absolute reactive cross sections by time-resolved reactant and product density measurements. The basic idea of this method is to utilize a well-defined source of OH to calibrate the obtained OH signal. In our experiment we used H_2O_2 photolysis at 193 nm as a reference. With the arrangement shown in Fig. 5 the distribution of OH radicals in the vibrational states $v=0,1$ over the rotational levels obtained by ArF-laser photolysis at 193 nm can be measured. The measured rotational distribution (see Fig. 7) is significantly hotter than that of earlier publications /23/. This is fundamentally due to the different conditions under which the OH spectra were taken. In /23/ an H_2O_2 pressure of 100 mTorr was reported whereas this work was carried out at a pressure of 5 mTorr of H_2O_2 . The delay between photolysis and probe-laser pulse was shortened by a factor of two. Rotational relaxation seems to be responsible for the partially relaxed distribution of OH quoted in /23/.

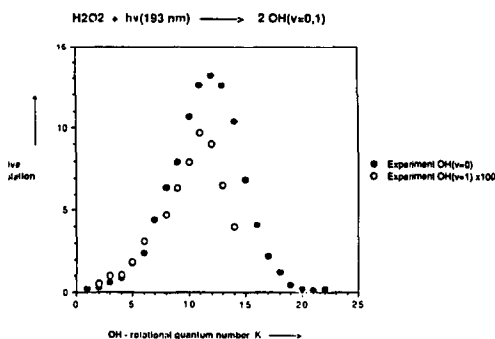


Fig. 7 Rotational distribution of OH ($^2\Pi$, $v=0,1$) after H_2O_2 photolysis at 193 nm

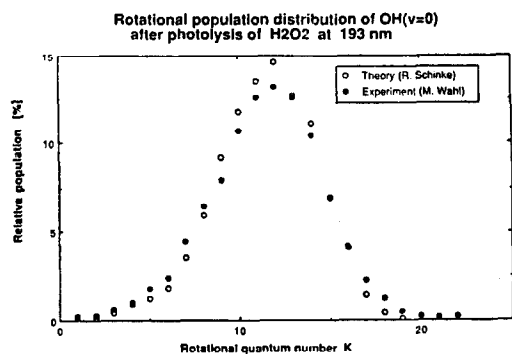


Fig. 8 Experimental and theoretical OH ($^2\Pi$, $v=0$) distribution after H_2O_2 photolysis at 193 nm

In several other photodissociation experiments, rotational distributions similar to ours were found. Sharply peaked Gaussian-like distributions do appear in OH after photolysis of H_2O_2 at 157 nm /24/, in NO after $(\text{CH}_3)_2\text{N}-\text{NO}$ photodissociation at 363.5 nm /25/, or in CO after photofragmentation of H_2CO /26/. Schinke /27/ recently introduced a semiclassical analysis of rotational distributions in photodissociation based on the sudden approximation. He described a method termed "angular reflection principle" which he used to calculate the CO rotational distribution of /26/, obtaining good agreement with experiment. As shown in Fig. 8 the OH rotational distribution after H_2O_2 photolysis is also a good example to test the validity of this theoretical approach.

The equation to calculate the absolute cross section given in ref. /22/ consists of several parameters, all readily measurable:

$$(I) \quad \sigma = \frac{[\text{OH}]_r^{\text{abs}} [\text{CH}_i]_{\text{H}_2\text{O}_2}^{\text{rel}}}{[\text{CH}_i]_{\text{H}_2\text{O}_2}^{\text{abs}} [\text{CH}_i]_{\text{H}_2\text{O}_2}^{\text{rel}}} \left\{ v_{\text{H}} [\text{CO}_2] t \frac{\sigma_{\text{HCl}} [\text{HCl}]}{\sigma_{\text{H}_2\text{O}_2} [\text{H}_2\text{O}_2]} \right\}^{-1}$$

where terms in brackets denote the concentration of the species usually given in cm^{-3} except for OH, which describes the LIF OH signal arising from excitation of state i and is given in arbitrary units. The indices "r" and " H_2O_2 " refer to signals measured after reaction and H_2O_2 photolysis, respectively and superscripts "abs" and "rel" refer to the absolute signal intensity (measured in au) and relative population in state i , $[\text{CH}_i]_{\text{rel}} = [\text{CH}_i] / \sum_j [\text{CH}_j]$. The velocity of the H atoms v_{H} was calculated from simple energy and momentum conservation to be 19060 ± 370 m/s. The delay t between photolysis and probe pulse was adjusted to 30–40 ns. During this time H atoms undergo approximately 0.1 collisions and OH less than 0.03 collisions with other species (HCl or CO_2). Absorption cross sections for HCl and H_2O_2 were interpolated from the literature for a photolysis wavelength of 193 nm and found to be correct within $\pm 10\%$ (193 nm: $\sigma_{\text{HCl}} = 9 \times 10^{-20} \text{ cm}^2 / 18,28/$, the absorption cross section for H_2O_2 of $6 \times 10^{-19} \text{ cm}^2 / 18,28/$ has to be corrected for a quantum yield of 1.76 ± 0.02 for production of $2\text{OH} / 29/$. Inserting all these values in eq. (I) we obtain for the total reactive cross section for the reaction of H atoms with CO_2 at a collision energy of 1.86 eV a value of $(0.4 \pm 0.2) \text{ \AA}^2$. As shown in Fig. 9 a significant increase is observed in the absolute reactive cross section if the collision energy increased to 2.6 eV. The result agrees well with extrapolation of relative cross section measurements by Wittig et al. /30/.

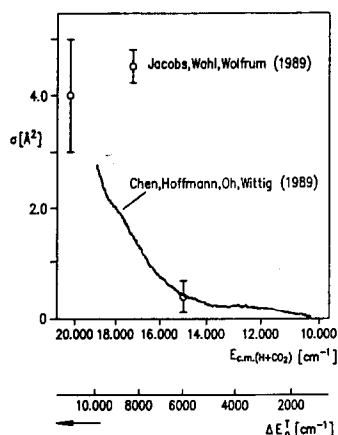


Fig. 9 Variation of the cross section of the reaction (-4) with relative translational energy at the reactants

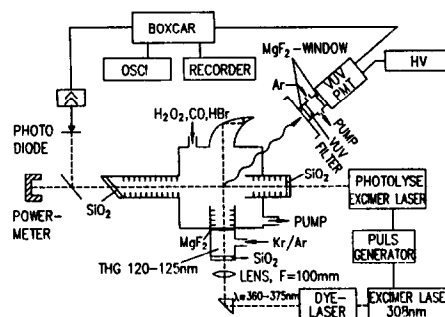


Fig. 10 Experimental arrangement for the time-resolved detection of H atoms produced in the reaction $\text{OH} + \text{CO} \rightarrow \text{CO}_2 + \text{H}$ by LIF in the vuv spectral region

Hydrogen atoms produced from the reaction of translationally hot, yet vibrationally cold OH radicals with CO were detected by laser-induced fluorescence using tunable VUV light in the region of the Lyman- α wavelength (s. Fig. 10). The VUV light was generated by frequency tripling /31/ the emission of an excimer laser-pumped dye laser tunable around 364 nm. The dye laser pulse of 20 mJ/cm^2 was focused by a quartz lens with $f = 10 \text{ cm}$ into a cell containing 400 torr of a krypton-argon mixture. The cell was separated from the reactor by an MgF_2 window. The fluorescence was detected with a solar blind multiplier (EMI G2CE 314) followed by a boxcar integrator (Stanford Research SR280). An interference filter (ARC 122N, 17% transmission at 121.8nm) was used in front of the multiplier to suppress the scattered light. The 90° arrangement of the two laser beams was chosen to reduce scattering from as well as damage of the MgF_2 window at the tripling cell by the photolysis laser. ⁵ At a total cell pressure of 90 mtorr, $v_{\text{OH}} = 4.7 \times 10^5 \text{ cm/sec} / 19/$ and a cross section of 60 \AA^2 , the probability of an OH radical undergoing more than one collision during the probe time of 60 ns is approximately 0.1, which allows almost collision free spectra to be recorded. The reaction cross section of reaction (4) is determined according to

$$\sigma \sim (v_{\text{OH}}) \frac{[\text{H}]_t}{[\text{OH}]_{t=0} [\text{CO}] v_{\text{OH}} t}$$

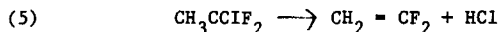
where v_{OH} is the velocity of the OH radicals after photolysis and t the probe time. The initial density of the OH reactant $[\text{OH}]_{t=0}$ is evaluated from the H_2O_2 partial pressure in the cell and its absorption cross section at 193 nm. The amount of H atoms produced in the reaction at time t $[\text{H}]_t$ is obtained by calibrating the H atom detection sensitivity via photolysis of HBr at 193 nm using $\sigma_{\text{HBr}} = 1.8 \times 10^{-18} \text{ cm}^2 / 32/$. The LIF signal of the product H atoms is displayed and compared to the calibration signal of H atoms from photolyzed HBr. The H atom signal from the photolysis of H_2O_2 at 193 nm /29/ has to be subtracted from the reaction signal. Evaluation of the nine best measurements yields a total reaction cross section of $19 \pm 10 \text{ \AA}^2$ at the center of mass collision energy of the experiment $E_{\text{c.m.}} = 1.32 \text{ eV}$.

3. LASER INDUCED RADICAL CHAIN REACTIONS

3.1 Kinetics of UV-laser Induced Dehydrochlorination of CH_2CClF_2

Vinylidene fluoride (vdf) is an important monomer used commercially for the production of polymers with special properties like high chemical and thermal stability. It is produced by

pyrolytic dehydrochlorination of 1-chloro-1,1-difluoroethane (cdfe) at temperatures of more than 800 K. Under these conditions cdfe is reacting by non-radical 4-center unimolecular step /33,34/



The concurrent elimination of HF /34/, which leads to severe corrosion problems in technical plants can be avoided by inducing a radical chain at lower temperatures. Huybrechts and Hubin /35,36/ have studied the thermal reaction of cdfe in the presence of CCl_4 and Cl_2 as radical initiators. A further increase of the reaction rate and a better defined formation² of radicals can be achieved by UV-laser photolysis /37/. For this purposes we have used a XeCl laser as a convenient light source, whose wavelength (308 nm) is near to the absorption maximum (328 nm) of molecular chlorine, which we added in small concentrations to the reactant for the photolytic generation of chlorine atoms /34/. The experimental data for the temperature dependence of HeCl_2 absorption cross section at 308 nm showed good agreement with theoretical values obtained by the method of Sulzer and Wieland /38/.

The quantum yield for the dehydrochlorination of cdfe was then determined by the concentration of the product vdf divided by the total amount of chlorine atoms produced in several laser pulses during the residence time of the reactor.

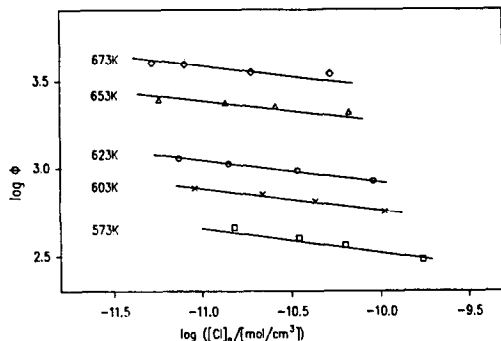


Fig. 11 Dependence of quantum yield for laser induced vdf formation on initial chlorine atom concentration. Cl_0 was modified by changing the XeCl laser energy

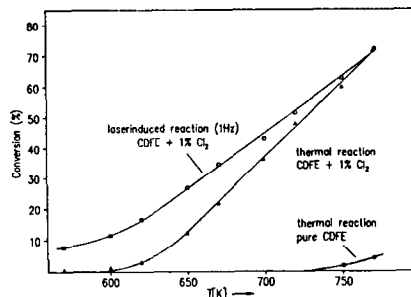
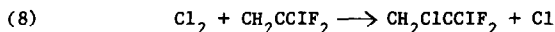
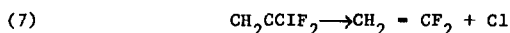
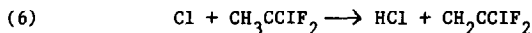


Fig. 12 Thermal and laser induced conversion of cdfe to vdf

Results of experiments, in which the energy density was varied by attenuating the laser beam, are shown in Fig. 11. Quantum yields in the range from 300 to 4000 decreased with rising initial concentration of chlorine atoms and decreased with temperature. Conversions from cdfe to vdf were reached 80%. As a side reaction cdfe was chlorinated to 1,2-dichloro-1,1-difluoroethane (dcdfc). The amount of dcdfc measured by gc analysis was proportional to the consumption of chlorine monitored by uv absorption. The radical chain leading to both products can be described by the initiation /34/ followed by the sequence:



We found that with the proceeding reaction the ratio of dehydrochlorination to chlorination is not a constant but is falling even at low conversions. This observation is in contrast to the work of Huybrecht and Hubin, who stated that the chlorination of vdf only starts at conversions of more than 5%. Arrhenius parameters for the two abstraction reactions (6) and



were determined by a competition method:

$$\log_{10}(k_6/\text{cm}^3 \text{ mol}^{-1} \text{ s}^{-1}) = (13.6 \pm 0.1) - (9200 \pm 300)/4.576T$$

$$\log_{10}(k_9/\text{cm}^3 \text{ mol}^{-1} \text{ s}^{-1}) = (13.7 \pm 0.1) - (6500 \pm 200)/4.576T$$

As a shown in Fig. 12 one can state that the photochemically induced radical chain reaction of 1-chloro-1,1-difluoroethane in the presence of chlorine is a suitable method for the production of the monomer vinylidene fluoride at temperatures much lower than common in the conventional industrial process.

3.2 CO₂-laser induced ignition of gas mixtures in cylindrical cells

The experiments on laser ignition were performed with gas mixtures composed of ozone and oxygen, e.g. the ozone decomposition flame. Light absorption of O₃ was used to monitor flame propagation in the UV-spectral range as well as to initiate the reaction by absorption of CO₂-laser pulses in the IR spectral range. Hence there was no need for additional sensitizers (e.g. SF₆) to absorb the laser light, the simple chemistry of the O₂-O₃ system was preserved. Fig. 13 shows schematically the experimental set-up described in detail in /40,41/. Light pulses of a TEA CO₂-laser operating at $\lambda = 9.552 \mu\text{m}$ in multimode oscillation were collimated to a beam waist of 2.7 mm width along the axis of a cylindrical vessel (diameter = 18 mm, length = 63 mm). The reaction was detected by UV light absorption on three paths perpendicular to the axis at the longitudinal positions = 12, 32 and 52 mm behind the entrance window. Fig. 13 shows the UV-light intensity transmitted in perpendicular and parallel detection paths.

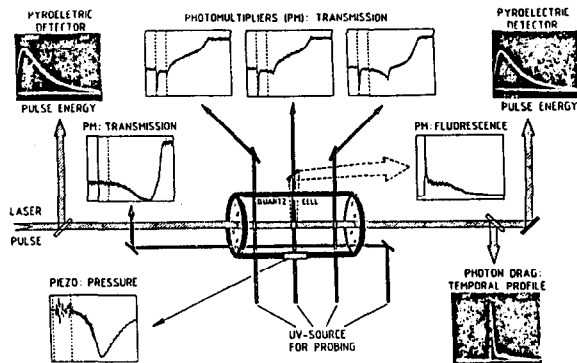


Fig. 13 The experimental method: laser excitation and ignition along the cell axis; probing of the incoming and outgoing laser energy by pyroelectric detectors; examination of the excitation process and the flame propagation on several probe beams via UV-light absorption of O₃; additional techniques: recording of the flame fluorescence, pressure traces and the temporal pulse profile

The absorbed CO₂-laser energy causes a steep decrease in the transmitted UV-light intensity due to the high ro-vibrational excitation produced in the O₃ molecules. This excitation relaxes into the remaining degrees of freedom of the gas mixture. The relaxation is reflected in an increase of the signal. A new thermal equilibrium is attained in the irradiated region of the cell. The corresponding intensity level is slightly lower than that before the laser pulse since the O₃ absorption rises strongly with increasing temperature /42/.

A typical simulation of ignition in an oxygen-ozone mixture is given in Fig. 14 /43/. After a relatively long induction period (confirming the corresponding experimental observation) there is a thermal explosion in the ignited gas pocket. This explosion initiates flame propagation across the vessel with subsequent equilibration by transport processes. To get an idea of the ozone deflagration near to ignition limit linearized ignition diagrams have been determined without consideration of shot to shot fluctuations. They have been deduced from the periods passing until the start and the end of the reaction on the various probe beams and from the average longitudinal and radial velocities. Fig. 14 shows an example for the behaviour near to the ignition limit. The deflagration starts and also proceeds slowly with a pronounced conical shape. In the case of higher fluence the flame front propagation usually becomes faster and nearly cylindrical symmetry is attained. Therefore, it is obvious that the behaviour of the macroscopic flame depends via the distribution of the laser heating in the beam waist region on the early processes of laser excitation and molecular relaxation. This feature is also important for the determination of the minimal ignition energy. The experiments accomplished so far revealed the existence of reproducible minimum of incoming as well as absorbed laser energy that brings about ignition for a given gas mixture.

The ignition process is simulated mathematically by solving the corresponding system of conservation equations. Spatial discretization using finite differences leads to a system of ordinary differential and algebraic equations which can be solved numerically. Due to the large ratio of vessel diameter to flame front thickness and to diameter of the artificial energy source adaptive gridding has to be used. Determination of the grid point density is done by equipartitioning the integral of a mesh function and inverse interpolation, the mesh function given by a weighted norm of temperature gradient and curvature. Piecewise monotone cubic Hermite interpolation is used for the static regridding /44-50/. The resulting systems of ordinary differential algebraic equations can be solved using the computer codes DASSL /51/ or LIMEX /52,53/.

Typical two-dimensional simulation for the ignition in an O₂/O₃ mixture for the evolution of temperature and pressure distributions using cylindrical symmetry are shown in Fig. 15.

Direct measurements of radial temperature profiles have been carried out by tunable IR-diode laser spectroscopy (see Fig. 16) using transient spectra of added CO molecules. By rapid scanning (10kHz) over the CO ($\nu=0, P2$) and CO ($\nu=1, R4$) lines temperature profiles at different radius distances have been obtained (s. Fig. 17).

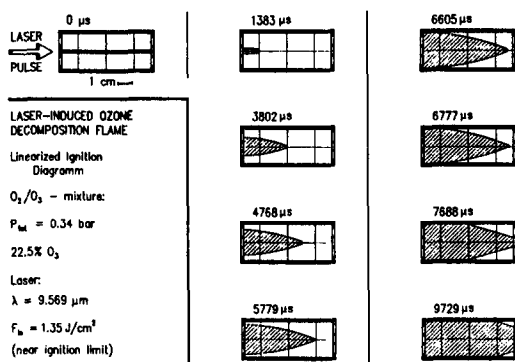


Fig. 14 Propagation of the flame front (hatched area = burnt gas) near the ignition limit

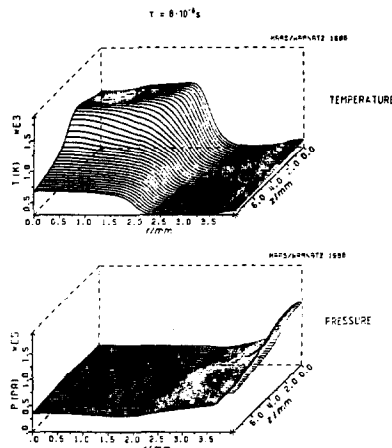


Fig. 15 2D-Simulation of CO₂-laser induced O₃/O₂ explosions

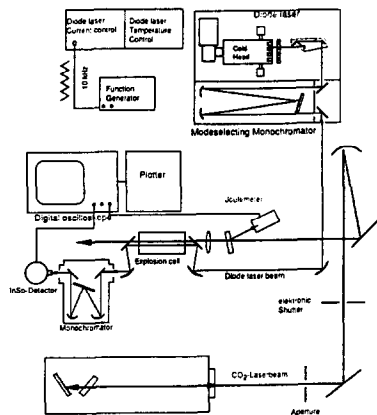


Fig. 16 Experimental setup for the investigation of CO₂ laser induced ignition processes by IR diode laser absorption spectroscopy

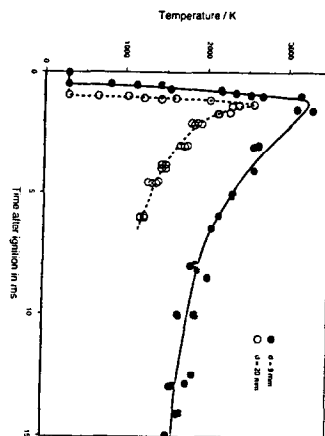


Fig. 17 Development of temperatures in the CO₂ laser induced ignition of CH₃OH (45%)/O₂ (50%)/CO (5%) mixtures

Literature

- /1/ S. Arrhenius, Z. Physik. Chem. 4, 226 (1889)
- /2/ F. London, Z. Elektrochem. Angew. Phys. Chem. 35, 592 (1929)
- /3/ P. Siegbahn, B. Liu, J. Chem. Phys. 68, 2455 (1978); 80, 581 (1984)
- /4/ J. Arnold, D. Chandler, Th. Dreier, Chemical Physics 133 123 (1989)
- /5/ W. Meier, G. Ahlers, H. Zacharias, J. Chem. Phys. 85, 2599 (1986)
- /6/ T. Dreier, J. J. Wolfrum, Int. J. of Chem. Kin. 18, 919 (1986)
- /7/ J.E. Spencer, H. Endo, G.P. Glass, 16th Symp. (Int.) on Combustion (Pittsburgh), 829 (1977)
- /8/ Th. Dreier, J. Wolfrum, 18th Symp. (Int.) on Combustion, The Combustion Institute, Pittsburgh, 801 (1981)
- /9/ G.A. Oldershaw, D.A. Potter, Nature 223, 490 (1969)
- /10/ R.E. Tomalesky, J.E. Sturm, J. Chem. Soc. Faraday Trans. II 68, 1241(1972)
- /11/ C.R. Quick, R.E. Weston, G.W. Flynn, Chem. Phys. Lett. 83, 15 (1981)
- /12/ F. Magnotta, D.J. Nesbitt, S.R. Leone, Chem. Phys. Lett. 83, 21 (1981)
- /13/ C.R. Quick, J.J. Tise, Chem. Phys. Lett. 100, 223 (1983)
- /14/ K. Kleinermanns, J. Wolfrum, Chem. Phys. Lett. 104, 157 (1984)
- /15/ K. Kleinermanns, E. Linnebach, J. Wolfrum, J. Phys. Chem. 89, 2525 (1985)
- /16/ S. Buelow, G. Radhakrishnan, J. Catanzarite, C. Wittig, J. Chem. Phys. 83, 444 (1985)
- /17/ J. Rice, G. Hoffmann, C. Wittig, J. Chem. Phys. 88, 2841 (1987)

- /17/ N.F. Scherer, L.R. Khundkar, R.B. Bernstein, A.H. Zewail, *Science* 242, 1645 (1988);
A.H. Zewail, *Science* 242, 1645 (1988)
- /18/ G.W. Flynn, R.E. Weston Jr., *Ann. Rev. Phys. Chem.* 37, 551 (1986)
G.W. Flynn, *Science* (to be published 1989)
- /19/ A. Jacobs, M. Wahl, R. Weller, J. Wolfrum, *Appl. Phys. B* 42, 173 (1987)
- /20/ M.H. Alexander et al. *J. Chem. Phys.* 89, 1749 (1988)
- /21/ K. Kleineremanns, E. Linnebach, M. Pohl, *J. Chem. Phys.* (in press)
- /22/ K. Kleineremanns, J. Wolfrum, *Appl. Phys. B* 34, 5 (1984); *J. Chem. Phys.* 80, 1446 (1984)
- /23/ G. Ondrey, N. van Veen, R. Bersohn, *J. Chem. Phys.* 78, 3732 (1983)
- /24/ H. Gölzenleuchter, K.H. Gericke, F.J. Comes, P.F. Linde, *Chem. Phys.* 89, 93 (1984)
- /25/ M. Dubs, U. Brühlmann, J.R. Huber, *J. Chem. Phys.* 84, 3106 (1986)
- /26/ D.J. Bamford, S.V. Filseth, M.F. Foltz, J.W. Hepburn, C.B. Moore, *J. Chem. Phys.* 82, 3032 (1985)
- /27/ R. Schinke, *J. Phys. Chem.* 90, 1742 (1986)
- /28/ W.B. DeMore, M.J. Molina, S.P. Sander, D.M. Golden, R.F. Hampson, M.J. Kurylo, C.J. Howard, A.R. Ravishankara, *Evaluation No. 8 of the NASA Panel for Data Evaluation*, JPL Publication 87, 41 (1987)
- /29/ U. Gerlach-Meyer, E. Linnebach, K. Kleineremanns, J. Wolfrum, *Chem. Phys. Lett.* 133, 113 (1987)
- /30/ Y. Chen, G. Hoffmann, D. Oh, C. Wittig, *Chem. Phys. Lett.* 159, 426 (1989)
- /31/ R. Schmidle, H. Dugan, W. Meier, K.H. Welge, *Z. Physik A* 304, 173 (1982)
- /32/ B.J. Huebert, R.M. Martin, *J. Phys. Chem.* 72, 3036 (1968)
- /33/ Yu. K. Panshin, N.G. Panshina, *Russ. J. Phys. Chem.* 44, 783 (1970)
- /34/ G.J. Martens, M. Godfroid, R. Decelle, J. Verbeyst, *Int. J. Chem. Kinet.* 4, 645 (1972)
- /35/ G. Huybrecht, Y. Hubin, *Int. J. Chem. Kin.* 17, 157 (1985)
- /36/ G. Huybrechts, Y. Hubin, *Int. J. Chem. Kin.* 18, 497 (1986)
- /37/ M. Schneider, J. Wolfrum, *Ber. Bunsenges. Phys. Chem.* 90, 1058 (1986)
- /38/ P. Sulzer, K. Wieland, *Helv. Phys. Acta*, 25, 653 (1952)
- /39/ J. Wolfrum, M. Schneider, *SPIE* 458, 82 (1984)
- /40/ B. Raffel, J. Warnatz, J. Wolfrum, *Appl. Phys. B* 37, 189 (1985)
- /41/ B. Raffel, J. Wolfrum, *Ber. Bunsenges. Phys. Chem.* 90, 997 (1986)
- /42/ D.C. Astholz, A.E. Croce, J. Troe, *J. Phys. Chem.* 86, 696 (1982)
- /43/ B. Raffel, J. Wolfrum, *Z. Phys. Chem., Neue Folge* 161, 43 (1989)
U. Maas, J. Warnatz, *Z. Phys. Chem. Neue Folge* 161, 61 (1989)
- /44/ R.J. Kee, J. Warnatz, J.A. Miller, "A Fortran Program Computer Code for the Evaluation of Gas-Phase Viscosities Conductivities and Diffusion Coefficients". SANDIA Report SAND83-8209 (1983)
- /45/ R.J. Kee, G. Dixon-Lewis, J. Warnatz, M.E. Coltrin, J.A. Miller, "A Fortran Computer Code for the Evaluation of Gas-Phase Multicomponent Transport Properties". SANDIA Report SAND86-8246 (1986)
- /46/ J. Warnatz, *Ber. Bunsenges. Phys. Chem.* 82, 193 (1978)
- /47/ N. Peters, J. Warnatz (Eds.), *Numerical Methods in Laminar Flame Propagation*. Vieweg. Braunschweig (1982)
- /48/ F.N. Fritsch, J. Butland, *J. Sci. Stat. Comput.* 5, 300 (1984)
- /49/ K.H. Ebert, P. Deuflhard, W. Jäger (Eds.), *Modelling of Chemical Reaction Systems*. Springer, Heidelberg (1981)
- /50/ J. Warnatz, W. Jäger (Eds.), *Complex Chemical Reaction Systems: Mathematical Modelling and Simulation*. Springer, Heidelberg (1987)
- /51/ L.R. Petzold, A Description of DASSL: A Differential/Algebraic System Solver, Sandia Report SAND82-8637. Sandia National Laboratories, Livermore (1982); IMACS World Congress, Montreal (1982)
- /52/ P. Deuflhard, E. Hairer, J. Zugck, *One-Step and Extrapolation Methods for Differential/Algebraic Systems*. Univ. Heidelberg, SFB 123: Tech. Rep. 318 (1985)
- /53/ P. Deuflhard, U. Nowak, *Extrapolation Integrators for Quasi-Linear Implicit ODEs*. Univ. Heidelberg, SFB 123: Tech. Rep. 332 (1985)